

WASP-32b: A transiting “hot Jupiter” planet orbiting a lithium-poor, solar-type star.

P.F.L. Maxted¹, D.R. Anderson¹, A. Collier Cameron², M. Gillon³, C. Hellier¹, D. Queloz⁴, B. Smalley¹, A.H.M.J. Triaud⁴, R.G. West⁵, R. Enoch², T.A. Lister⁶, F. Pepe⁴, D.L. Pollacco⁷, D. Ségransan⁴, I. Skillen⁸, S. Udry⁴

ABSTRACT

We report the discovery of a transiting planet orbiting the star TYC 2-1155-1. The star, WASP-32, is a moderately bright ($V=11.3$) solar-type star ($T_{\text{eff}} = 6100 \pm 100$ K, $[\text{Fe}/\text{H}] = -0.13 \pm 0.10$). The lightcurve of the star obtained with the WASP-South and WASP-North instruments shows periodic transit-like features with a depth of about 1% and a duration of 0.10 d every 2.72 days. The presence of a transit-like feature in the lightcurve is confirmed using z-band photometry obtained with Faulkes Telescope North. High resolution spectroscopy obtained with the CORALIE spectrograph confirms the presence of a planetary mass companion. From a combined analysis of the spectroscopic and photometric data, assuming that the star is a typical main-sequence star, we estimate that the planet has a mass M_{p} of $3.60 \pm 0.07 M_{\text{Jup}}$ and a radius $R_{\text{p}} = 1.19 \pm 0.06 R_{\text{Jup}}$. WASP-32 is one of a small group of “hot Jupiters” with masses $> 3 M_{\text{Jup}}$. We find that some stars with hot Jupiter companions and with masses $M_{\star} \approx 1.2 M_{\odot}$, including WASP-32, are depleted in lithium, but that the majority of these stars have similar lithium abundances to field stars.

Subject headings: planetary systems

¹Astrophysics Group, Keele University, Staffordshire, ST5 5BG, UK

²School of Physics and Astronomy, University of St. Andrews, North Haugh, Fife, KY16 9SS, UK

³Institut d’Astrophysique et de Géophysique, Université de Liège, Allée du 6 Août, 17, Bat. B5C, Liège 1, Belgium

⁴Observatoire de Genève, Université de Genève, 51 Chemin des Maillettes, 1290 Sauverny, Switzerland

⁵Department of Physics and Astronomy, University of Leicester, Leicester, LE1 7RH, UK

⁶Las Cumbres Observatory, 6740 Cortona Dr. Suite 102, Santa Barbara, CA 93117, USA

⁷Astrophysics Research Centre, School of Mathematics & Physics, Queen’s University, University Road, Belfast, BT7 1NN, UK

⁸Isaac Newton Group of Telescopes, Apartado de Correos 321, E-38700 Santa Cruz de la Palma, Tenerife, Spain

1. Introduction

The WASP project (Pollacco et al. 2006) is currently one of the most successful wide-area surveys designed to find exoplanets transiting relatively bright stars. Other successful surveys include HATnet (Bakos et al. 2004), XO (McCullough et al. 2005) and TrES (O’Donovan et al. 2006). The Kepler satellite is now also starting to find many transiting exoplanets (Borucki et al. 2010). There is continued interest in finding transiting exoplanets because they can be accurately characterized and studied in some detail, e.g., the mass and radius of the planet can be accurately measured. This gives us the opportunity to explore the relationships between the density of the planet and other properties of the planetary system, e.g., the semi-major axis, the composition and spectral type of the star, etc. Given the wide variety of transiting planets being discovered and the large number of parameters that characterize them, statistical studies will require a large sample of systems to identify and quantify the relationships between these parameters. These relationships can be used to test models of the formation, structure and evolution of short period exoplanets. Here we report the discovery of a “hot Jupiter” companion to the star WASP-32 and show that this star is lithium poor compared to other stars of similar mass.

2. Observations

The two WASP instruments each consist of an array of 8 cameras with Canon 200-mm f/1.8 lenses and 2k×2k *e2V* CCD detectors providing image with a field-of-view of $7.8^\circ \times 7.8^\circ$ at an image scale of 13.7 arcsec/pixel (Pollacco et al. 2006; Wilson et al. 2008). The star TYC 2-1155-1 (= 1SWASP J001550.81+011201.5) was observed 5906 times in one camera of the WASP-South instrument in Sutherland, South Africa during the interval 2008 June 30 to 2008 Nov 17. Our transit detection algorithm (Collier Cameron et al. 2007) identified a periodic feature with a depth of approximately 0.01 magnitudes recurring with a 2.72-d period in these data. The width and depth of the transit are consistent with the hypothesis that it is due to a planet with a radius of approximately 1 Jupiter radius orbiting a solar-type star. The proper motion and catalogue photometry available for TYC 2-1155-1 suggest that it is a mid-F type, main-sequence star. We therefore added this star to our programme of follow-up observations for candidate planet host stars.

A further 4156 observations of TYC 2-1155-1 were secured with WASP-South in the interval 2009 June 28 to 2009 Nov 18. TYC 2-1155-1 was also observed by the WASP-North instrument 2687 times during the interval 2008 August 4 to 2008 November 30 and 4308 times during the interval 2009 August 5 to 2009 Oct 20. All these data are shown as a function of phase in Fig. 1. ¹

We obtained 15 radial velocity measurements of WASP-32 during the interval 2009 September

¹All photometric data presented in this paper are available from the NStED database².

1 to 2009 December 22 with the CORALIE spectrograph on the Euler 1.2-m telescope located at La Silla, Chile (Table 1). The amplitude of the radial velocity variation with the same period as the transit lightcurve (Fig. 2) and the lack of any correlation between this variation and the bisector span establish the presence of a planetary mass companion to this star (Queloz et al. 2001).

We obtained photometry further photometry of TYC 2-1155-1 and other nearby stars on 2009 December 7 using the fs03 Spectral camera on the LCOGT 2.0-m Faulkes Telescope North (FTN) at Haleakala, Maui in order to better define the depth and width of the transit signal. The Spectral camera used a 4096×4096 pixel Fairchild CCD with $15 \mu\text{m}$ pixels which were binned 2×2 giving an image scale of $0.303 \text{ arcsec/pixel}$ and a field-of-view of $10' \times 10'$. We used a Pan-STARRS z filter to obtain 187 images covering one egress of the transit. These images were pre-processed using the WASP Pipeline (Pollacco et al. 2006) using a combined bias and flat frame and the DAOPHOT photometry package (Stetson 1987) was used within the IRAF³ environment to perform object detection and aperture photometry with an aperture size of 9 binned pixels in radius. Differential magnitudes were derived by combining the flux of 11 stable comparison stars that were within the instrumental field-of-view. The resulting lightcurve is shown in Fig. 3. The coverage of the out-of-transit phases is quite limited, but the data are sufficient to confirm that transit-like features seen in the WASP data are due to the star TYC 2-1155-1 and to provide precise measurements of the depth of the transit and the duration of egress.

3. WASP-32 Stellar Parameters

The 15 individual CORALIE spectra of WASP-32 were co-added to produce a single spectrum with an approximate signal-to-noise ratio of around 80:1. The standard pipeline reduction products were used in the analysis.

The analysis was performed using the methods given in Gillon et al. (2009b). The H_α line was used to determine the effective temperature (T_{eff}), while the Na I D and Mg I b lines were used as surface gravity ($\log g$) diagnostics. The elemental abundances were determined from equivalent width measurements of several clean and unblended lines. Atomic line data was mainly taken from the Kurucz and Bell (1995) compilation, but with updated van der Waals broadening coefficients for lines in Barklem et al. (2000) and $\log gf$ values from Gonzalez and Laws (2000), Gonzalez et al. (2001) or Santos et al. (2004). Individual lines abundances were determined from the measured equivalent widths. The mean values relative to solar are given in Table 2.

A value for microturbulence (ξ_t) was determined from the Fe I lines using Magain’s (1984) method. The quoted error estimates include that given by the uncertainties in T_{eff} , $\log g$ and ξ_t , as well as the scatter due to measurement and atomic data uncertainties.

³IRAF is distributed by the National Optical Astronomy Observatory, which is operated by the Association of Universities for Research in Astronomy (AURA) under cooperative agreement with the National Science Foundation.

The projected stellar rotation velocity ($v \sin i$) was determined by fitting the profiles of several unblended Fe I lines. A value for macroturbulence (v_{mac}) of $4.7 \pm 0.3 \text{ km s}^{-1}$ was assumed, based on the tabulation by Gray (2008), and an instrumental FWHM of $0.11 \pm 0.01 \text{ \AA}$, determined from the telluric lines around 6300 \AA . A best fitting value of $v \sin i = 4.8 \pm 0.8 \text{ km s}^{-1}$ was obtained.

3.1. Planetary parameters

The CORALIE radial velocity measurements were combined with the WASP-South, WASP-North and FTN z-band photometry in a simultaneous Markov-chain Monte-Carlo (MCMC) analysis to find the parameters of the WASP-32 system. The shape of the transit is not well defined by the available photometry, so we have imposed an assumed main-sequence mass–radius relation as an additional constraint in our analysis of the data. The stellar mass is determined from the parameters T_{eff} , $\log g$ and $[\text{Fe}/\text{H}]$ using the procedure described by Enoch et al. (2010). The code uses T_{eff} and $[\text{Fe}/\text{H}]$ as MCMC jump variables, constrained by Bayesian priors based on the spectroscopically-determined values given in Table 2. The parameters derived from our MCMC analysis are listed in Table 3.

Note that in contrast to previous analyses of this type, we now use the parameters $\sqrt{e \cos \omega}$ and $\sqrt{e \sin \omega}$ in the MCMC analysis. This removes a bias in the analysis towards larger values of e , i.e., using $e \cos \omega$ and $e \sin \omega$ effectively imposes a prior probability distribution for $e \propto e^2$, whereas using $\sqrt{e \cos \omega}$ and $\sqrt{e \sin \omega}$ is equivalent to a uniform prior for e . Nevertheless, the MCMC solution suggests a marginal detection of a non-zero orbital eccentricity (2.8σ). This result can be confirmed by measuring the phase of the secondary eclipse, which is expected to be displaced from phase 0.5 by 40 minutes given our best estimate of $e \cos \omega$.

The chi-squared value of the fit to our 15 radial velocity measurements is $\chi_{\text{rv}}^2 = 16.7$. There are 6 free parameters; P and T_0 are determined almost entirely by the lightcurves, K and γ are determined entirely by the radial velocity data but e and ω are constrained by both data sets. The number of degrees of freedom is $N_{\text{df}} \approx 15 - 3 = 12$. We did not consider it necessary to increase the standard errors of the radial velocity data to account for external noise due to stellar activity (“jitter”) since $\chi_{\text{rv}}^2 \approx N_{\text{df}}$. The $\log g$ value derived from our MCMC solution is consistent with the $\log g$ value from the analysis of the spectrum, although this is a rather weak constraint because the $\log g$ value from the analysis of the spectrum has a much larger uncertainty.

4. Discussion and Conclusions

Of the 69 transiting planets currently known with directly measured masses, only 11 (including WASP-32 b) have masses greater than $3 M_{\text{Jup}}$.⁴ The discovery of WASP-32 b will improve our understanding of how the properties of hot Jupiters vary with the planet’s mass.

Israelian et al. (2009) claim that, on average, stars with planets have a lower lithium abundance than normal solar-type stars in the effective temperature range of 5600 – 5900 K. Sousa et al. (2010) claim that this result was not a consequence of the distribution of age or mass of the planet host stars. Both these claims have been disputed by Baumann et al. (2010) who find that the apparent connection between lithium abundance and the presence of an exoplanet in the sample of Israelian et al. can be explained by subtle biases in their sample. Israelian et al. did not identify any peculiarities in the pattern of lithium abundance for planet-host stars with $T_{\text{eff}} \gtrsim 5850$ K. The trend of lithium abundance becomes more complex when these hotter, more massive stars are considered. The relation between mass and T_{eff} also depends on the age and metallicity of the star so the trend is only seen clearly if plotted as a function of mass, not T_{eff} .

For field stars with accurate parallaxes, T_{eff} , $[\text{Fe}/\text{H}]$ and $\log g$ measurements, the mass of the star can be estimated by comparison with stellar models. Lambert and Reddy (2004) estimated the mass of 451 F-G stars using this method and compared their surface lithium abundance to similar stars in various open clusters. Their trend of lithium abundance versus mass for Hyades stars is shown in Fig. 4 together with their results for F-G stars with $[\text{Fe}/\text{H}] > -0.2$. The location of the prominent dip in the lithium abundance near masses of $1.4 M_{\odot}$ moves to lower masses for stars with lower metallicities. The upper limit $T_{\text{eff}} \approx 5850$ K used by Israelian et al. (2009) corresponds to a mass of approximately $1.1 M_{\odot}$.

Also shown in Fig. 4 are the measured lithium abundances for the transiting hot Jupiter systems listed in Table 4. Stellar masses for WASP planets in Table 4 have been re-calculated using the method of Enoch et al. (2010) using the data specified in the reference provided, unless otherwise noted. The metallicities of these stars are similar to the field stars shown in this figure. The tendency suggested by Israelian et al. (2009) for planet host stars with masses $\lesssim 1.1 M_{\odot}$ to be lithium poor is also seen to be present for transiting hot Jupiter planets. However, as Baumann et al. (2010) have shown, this tendency may be a consequence of the age and metallicity distribution of the samples and be unconnected to the presence or absence of a planetary companion.

For more massive hot Jupiter systems there are a few hot Jupiter systems that are strongly lithium depleted, but the majority of these more massive host stars have similar lithium abundances to field F-G stars. The position of WASP-32 in this diagram shows that there is a continuous range of lithium depletion for planet-host stars with masses of about $1.2 M_{\odot}$. There is no obvious correlation between the properties of the stars or their planets and the degree of lithium depletion.

⁴<http://exoplanet.eu>

A more detailed analysis of this issue would benefit from a homogeneous set of age and metallicity estimates for the host stars of hot Jupiter planets.

WASP-South is hosted by the South African Astronomical Observatory and we are grateful for their ongoing support and assistance. Funding for WASP comes from consortium universities and from the UKs Science and Technology Facilities Council. M. Gillon acknowledges support from the Belgian Science Policy Office in the form of a Return Grant

REFERENCES

- Anderson, D. R. et al. 2010, *ApJ*, 709, 159
- Anderson, D. et al. 2010a, in prep.
- Bakos, G., Noyes, R. W., Kovács, G., Stanek, K. Z., Sasselov, D. D., and Domsa, I. 2004, *PASP*, 116, 266
- Barklem, P. S., Piskunov, N., and O’Mara, B. J. 2000, *A&AS*, 142, 467
- Baumann, P., Ramírez, I., Meléndez, J., Asplund, M., and Lind, K. 2010, *ArXiv e-prints*
- Borucki, W. J. et al. 2010, *Science*, 327, 977
- Bouchy, F. et al. 2010, *ArXiv e-prints*
- Collier Cameron, A. et al. 2007, *MNRAS*, 380, 1230
- Enoch, B., Collier Cameron, A., Parley, N. R., and Hebb, L. 2010, *A&A*, 516, A33
- Enoch, B. et al. 2010a, in prep.
- Gillon, M. et al. 2009a, *A&A*, 501, 785
- Gillon, M. et al. 2009b, *A&A*, 496, 259
- Gonzalez, G. and Laws, C. 2000, *AJ*, 119, 390
- Gonzalez, G., Laws, C., Tyagi, S., and Reddy, B. E. 2001, *AJ*, 121, 432
- Hebb, L. et al. 2010, *ApJ*, 708, 224
- Hellier, C. et al. 2009a, *Nature*, 460, 1098
- Hellier, C. et al. 2009b, *ApJ*, 690, L89
- Israelian, G. et al. 2009, *Nature*, 462, 189

- Joshi, Y. C. et al. 2009, MNRAS, 392, 1532
- Kurucz, R. L. and Bell, B. (eds.) 1995, Atomic line list, Kurucz CD-ROM No. 23. Cambridge, Mass.: Smithsonian Astrophysical Observatory.
- Lambert, D. L. and Reddy, B. E. 2004, MNRAS, 349, 757
- Lister, T. A. et al. 2009, ApJ, 703, 752
- Maxted, P. F. L. et al. 2010, ArXiv e-prints
- McCullough, P. R., Stys, J. E., Valenti, J. A., Fleming, S. W., Janes, K. A., and Heasley, J. N. 2005, PASP, 117, 783
- Melo, C., Santos, N. C., Pont, F., Guillot, T., Israelian, G., Mayor, M., Queloz, D., and Udry, S. 2006, A&A, 460, 251
- O’Donovan, F. T., Charbonneau, D., and Hillenbrand, L. 2006, in Bulletin of the American Astronomical Society, Vol. 38, Bulletin of the American Astronomical Society, p. 1212
- Pollacco, D. et al. 2008, MNRAS, 385, 1576
- Pollacco, D. L. et al. 2006, PASP, 118, 1407
- Pollacco, D. et al. 2010, in prep.
- Queloz, D. et al. 2001, A&A, 379, 279
- Queloz, D. et al. 2010, A&A, 517, L1
- Santos, N. C., Israelian, G., and Mayor, M. 2004, A&A, 415, 1153
- Santos, N. C. et al. 2006, A&A, 450, 825
- Skillen, I. et al. 2009, A&A, 502, 391
- Smalley, B. et al. 2010, ArXiv e-prints
- Smalley, B. et al. 2010b, in prep.
- Sousa, S. G., Fernandes, J., Israelian, G., and Santos, N. C. 2010, A&A, 512, L5
- Southworth, J. 2009, MNRAS, 394, 272
- Sozzetti, A. et al. 2009, ApJ, 691, 1145
- Stetson, P. B. 1987, PASP, 99, 191
- Street, R. A. et al. 2010, ApJ, 720, 337

Torres, G., Winn, J. N., and Holman, M. J. 2008, *ApJ*, 677, 1324

West, R. G. et al. 2009, *AJ*, 137, 4834

West, R. et al. 2010, in prep.

Wilson, D. M. et al. 2008, *ApJ*, 675, L113

Table 1: Radial velocity measurements of the star WASP-32. The standard error of the bisector span measurements, BS, is $2\sigma_{RV}$.

BJD	RV	σ_{RV}	BS
–2 450 000	(km s ^{–1})	(km s ^{–1})	(km s ^{–1})
5075.8412	17.883	0.019	0.008
5117.6744	18.922	0.123	0.088
5125.6262	18.674	0.018	0.041
5126.6901	18.147	0.015	–0.027
5127.6192	17.980	0.014	0.009
5127.7019	18.003	0.016	0.018
5128.6424	18.761	0.015	0.024
5128.6669	18.739	0.018	0.090
5129.5810	17.976	0.016	0.003
5129.6984	17.866	0.016	–0.022
5179.5626	18.271	0.014	0.015
5180.5828	18.641	0.012	0.052
5181.5665	17.805	0.013	0.060
5185.5560	18.739	0.015	0.055
5188.5509	18.773	0.019	0.063

Table 2: Stellar parameters of WASP-32 from Spectroscopic Analysis.

Parameter	Value
T_{eff} (K)	6100 ± 100
$\log g$	4.4 ± 0.2
ξ_t (km s ^{–1})	1.2 ± 0.1
$v \sin i$ (km s ^{–1})	4.8 ± 0.8
[Fe/H]	-0.13 ± 0.10
[Si/H]	-0.06 ± 0.10
[Ca/H]	-0.02 ± 0.12
[Ti/H]	-0.07 ± 0.10
[Cr/H]	-0.10 ± 0.09
[Ni/H]	-0.16 ± 0.08
$\log A(\text{Li})$	1.58 ± 0.11

Table 3: System parameters for WASP-32. The planet equilibrium temperature, T_P , is calculated assuming a value for the Bond albedo $A=0$. **N.B.** an assumed main-sequence mass-radius relation is imposed as an additional constraint in this solution so the mass and radius of the star are not independent parameters – see Collier Cameron et al. (2007) for details.

Parameter (Unit)	Value	Notes
P (d)	2.718659 ± 0.000008	Orbital period
T_c (HJD)	2455151.0546 ± 0.0005	Time of mid-transit
T_{14} (d)	0.101 ± 0.002	Transit duration
T_{12} (d)	0.0161 ± 0.0015	Ingress duration
$\Delta F = R_P^2/R_*^2$	0.0124 ± 0.0004	
$b = a \cos(i)/R_*$	0.628 ± 0.004	
i ($^\circ$)	85.3 ± 0.5	Orbital inclination
K_1 (m s^{-1})	483 ± 6	Semi-amplitude of spectroscopic orbit
γ (m s^{-1})	18281 ± 1	Radial velocity of barycentre
$\sqrt{e \cos \omega}$	-0.12 ± 0.03	
$\sqrt{e \sin \omega}$	0.05 ± 0.07	
e	0.018 ± 0.0065	Orbital eccentricity
ω	160 ± 30	Longitude of periastron
M_* (M_\odot)	1.10 ± 0.03	Stellar mass
R_* (R_\odot)	1.11 ± 0.05	Stellar radius
$\log g_*$ (cgs)	4.39 ± 0.03	Logarithmic stellar surface gravity
ρ_* (ρ_\odot)	0.80 ± 0.10	Mean stellar density
M_P (M_{Jup})	3.60 ± 0.07	Planetary mass
R_P (R_{Jup})	1.18 ± 0.07	Planetary radius
$\log g_P$ (cgs)	3.77 ± 0.04	Logarithmic planetary surface gravity
ρ_P (ρ_J)	2.2 ± 0.4	Mean planetary density
a (AU)	0.0394 ± 0.0003	Semi-major axis of the orbit
T_P (K)	1560 ± 50	Planetary equilibrium temperature

Table 4. Lithium abundances and masses for planet host stars.

Star	Mass (M_{\odot})	$\log A(\text{Li})$	Refs.
HD189733	0.87 ± 0.05	< -0.1	1,2
HD209458	1.17 ± 0.04	2.7 ± 0.1	1,2
OGLE-TR-10	1.24 ± 0.05	2.3 ± 0.1	1,2
OGLE-TR-56	1.25 ± 0.06	2.7 ± 0.1	1,2
OGLE-TR-111	0.86 ± 0.07	< 0.51	1,2
OGLE-TR-113	0.78 ± 0.02	< 0.2	3,2
TrES-1	0.93 ± 0.05	< 0.5	1,2
WASP-1	1.28 ± 0.04	2.91 ± 0.05	1,4
WASP-2	0.88 ± 0.01	< 0.81	1,5
WASP-3	1.22 ± 0.09	2.25 ± 0.25	6
WASP-4	0.96 ± 0.036	< 0.79	7
WASP-5	1.02 ± 0.038	< 0.6	7
WASP-6	0.87 ± 0.07	< 0.5	8
WASP-7	1.19 ± 0.029	< 1.0	9
WASP-8	0.99 ± 0.024	1.5 ± 0.1	10
WASP-12	1.28 ± 0.041	2.46 ± 0.1	11
WASP-13	1.10 ± 0.030	2.06 ± 0.1	12
WASP-14	1.23 ± 0.033	2.84 ± 0.05	13
WASP-15	1.21 ± 0.034	< 1.2	14
WASP-16	1.01 ± 0.035	< 0.8	15
WASP-17	1.23 ± 0.040	< 1.3	16
WASP-18	1.21 ± 0.031	2.65 ± 0.08	17
WASP-19	0.97 ± 0.023	< 1.0	18
WASP-20	1.09 ± 0.025	2.40 ± 0.10	19
WASP-21	0.99 ± 0.025	2.19 ± 0.09	20
WASP-22	1.10 ± 0.025	2.23 ± 0.08	21
WASP-24	1.17 ± 0.028	2.45 ± 0.08	22
WASP-25	1.00 ± 0.030	1.63 ± 0.09	23
WASP-26	1.11 ± 0.027	1.90 ± 0.12	24
WASP-28	1.06 ± 0.028	2.52 ± 0.12	25
WASP-30	1.14 ± 0.027	2.95 ± 0.10	26
WASP-32	1.19 ± 0.030	1.58 ± 0.11	
WASP-34	1.06 ± 0.035	< 0.82	27

Table 4—Continued

Star	Mass (M_{\odot})	log A(Li)	Refs.
TrES-3	0.92 ± 0.04	< 1.0	28
TrES-4	1.39 ± 0.10	< 1.5	28

References. — 1. Southworth (2009); 2. Melo et al. (2006); 3. Torres et al. (2008); 4. Santos et al. (2006); 5. Smalley (priv. comm.); 6. Pollacco et al. (2008); 7. Gillon et al. (2009b); 8. Gillon et al. (2009a); 9. Hellier et al. (2009b); 10. Queloz et al. (2010); 11. Smalley (priv. comm.); 12. Skillen et al. (2009); 13. Joshi et al. (2009); 14. West et al. (2009); 15. Lister et al. (2009); 16. Anderson et al. (2010); 17. Hellier et al. (2009a); 18. Hebb et al. (2010); 19. Pollacco et al. (2010); 20. Bouchy et al. (2010); 21. Maxted et al. (2010); 22. Street et al. (2010); 23. Enoch et al. (2010); 24. Smalley et al. (2010); 25. West et al. (2010); 26. Anderson et al. (2010); 27. Smalley et al. (2010b); 28. Sozzetti et al. (2009)

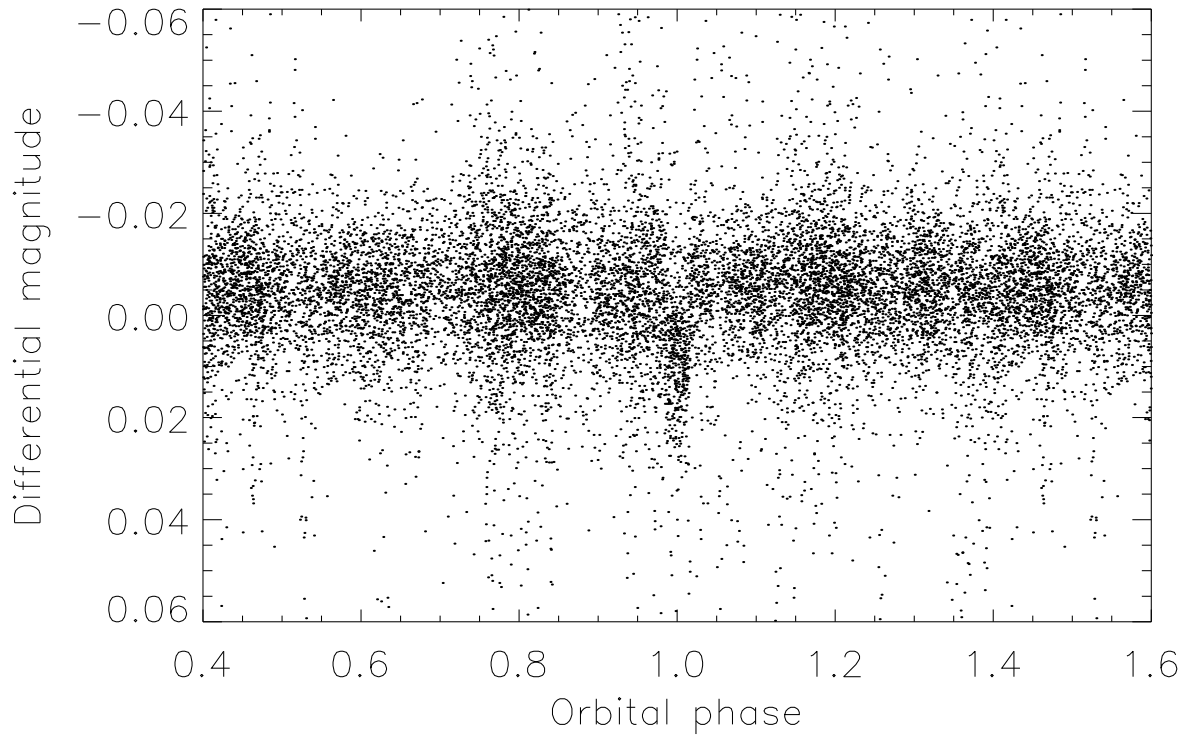


Fig. 1.— WASP photometry of WASP-32 folded on the orbital period $P = 2.71866$ d.

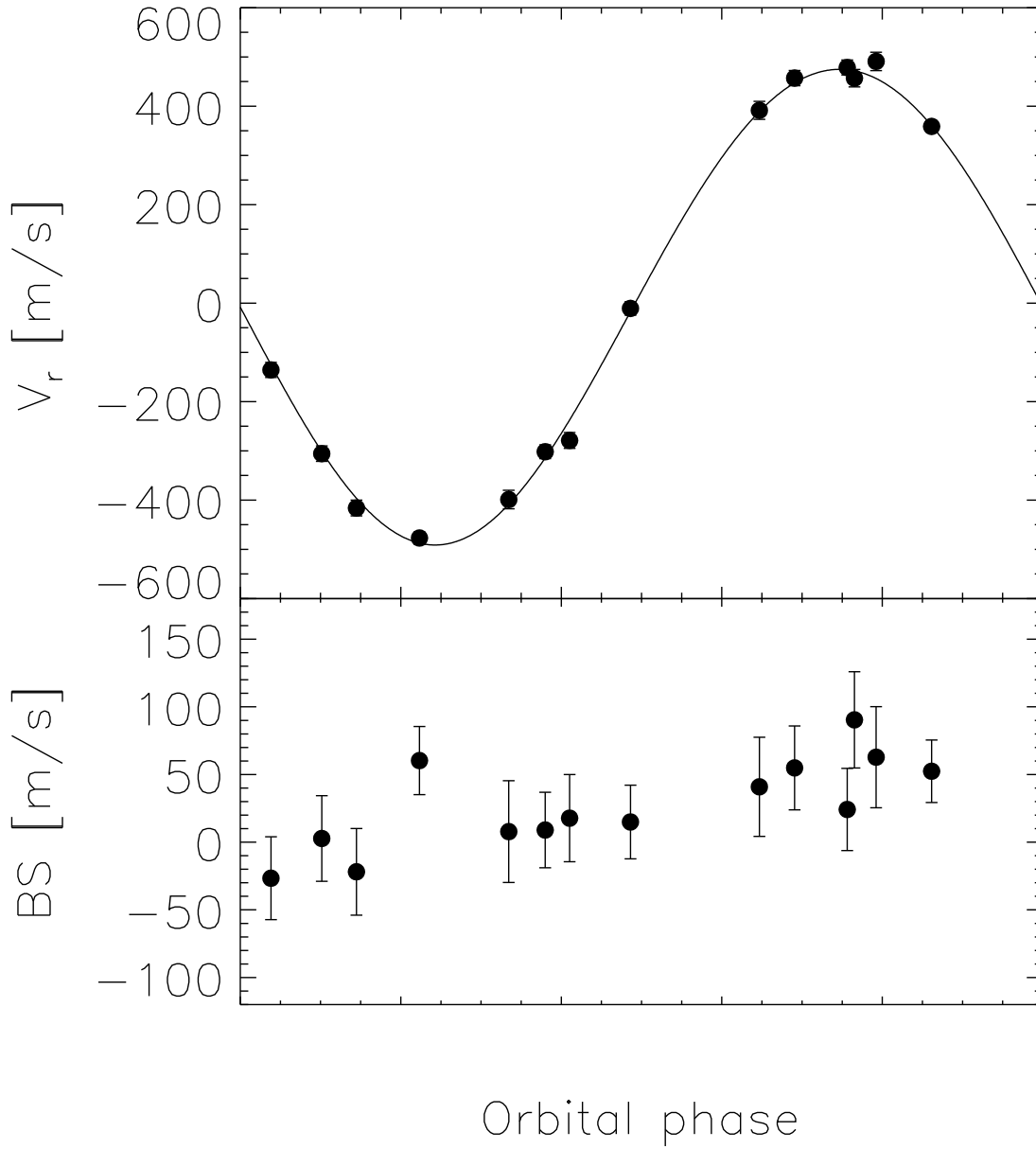


Fig. 2.— Radial velocity and bisector span measurements for WASP-32. Upper panel: Radial velocity data (points with error bars) with our model for the spectroscopic orbit (solid line). Lower panel: bisector span measurements. (One point with large error bars is not shown here).

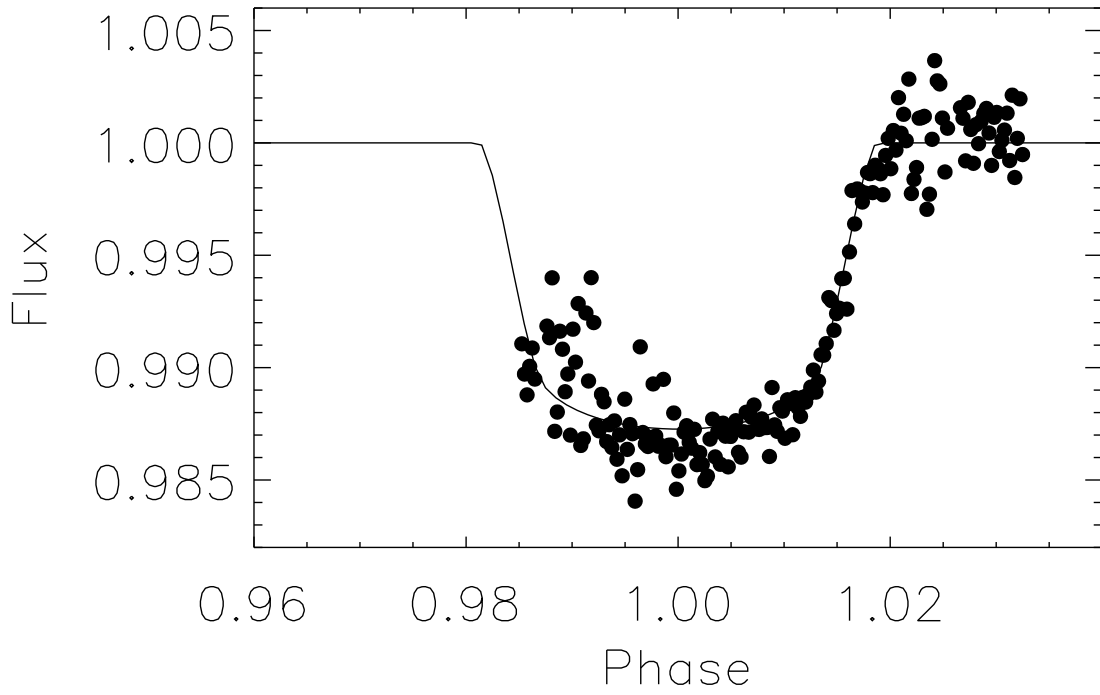


Fig. 3.— FTN z-band photometry of the transit of WASP-32 (points) together with a model lightcurve for our best-fitting model parameters (solid line).

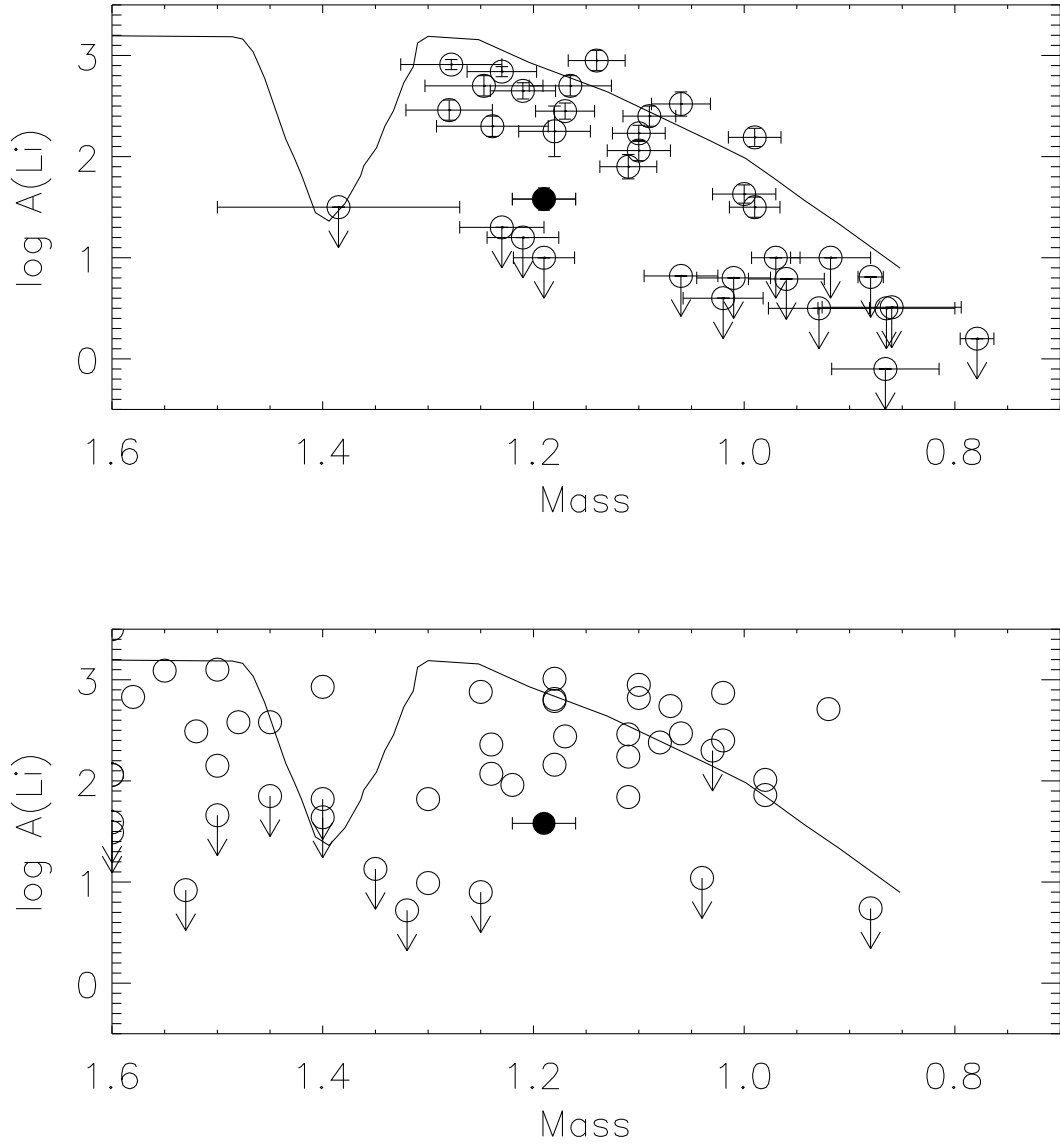


Fig. 4.— Upper panel: Lithium abundance as a function of stellar mass for transiting hot Jupiter planet host stars. Upper limits are indicated with downward pointing arrows. WASP-32 is plotted with a filled symbol. The solid line is the mean relation for the Hyades stars from Lambert and Reddy (2004). Lower panel: Lithium abundance for thin-disk stars with $[\text{Fe}/\text{H}] > -0.2$ from Lambert and Reddy.